Estimation of solar energy potential over Mongolia based on satellite data

Onon Bayasgalan[1,*], Amarbayar Adiyabat[1], Jun Hashimoto[2], Kenji Otani[2]

[1] *Department of Electronic and Communication Engineering, National University of Mongolia, Ulaanbaatar, Mongolia*
[2] *Energy Networking team, Fukushima Renewable Energy Institute, AIST, Fukushima, Japan*

Abstract —We aim to estimate solar resource of Mongolia using satellite data in combination with limited ground measurements. Visible channel images provided by Japanese Geostationary Meteorological Satellite (GMS) Himawari 8 are correlated with ground-based measurements of solar irradiation to derive parameters of the semi-physical model.

Keywords — Solar irradiance, Mongolia, semi-physical model, Himawari 8 GMS, ground measurement.

I. INTRODUCTION

Due to its climatic characteristics, Mongolia is listed as one of the countries with abundant renewable sources, especially, the southern part of the country, Gobi-desert area is a great location for solar and wind projects. According to the study conducted by International renewable energy agency (IRENA), there are approximately 270-300 clear sky days in a year with daily average solar energy of 3.4-5.4 kWh/m2/day [1]. However, due to the lack of a sufficient number of ground measurement stations in Mongolia, this potential is yet to be mapped.

In order to estimate solar irradiance, ground measurement, satellite data or their combination can be used. Ground measurement has high accuracy but when the distance between ground measurement stations is more than 25km, the interpolation method results in a high error. On the other hand, satellite data can cover a wide area but its temporal and spatial resolution is low [2]. In other words, ground data is pinpoint measurement integrated over time while satellite data is instantaneous measurement integrated over an area. Thus, in this study, ground measurement enhanced satellite data is used since they complement each other.

Similar studies have been conducted on a local and global scale with different types of models. J.Alonso-Montesinos et al derived all components of solar irradiance in 15 minutes interval from Meteosat 7 and 8 satellite of European Union (EU) by Heliosat 2 method for the period of 2010 to 2014. Sky condition is classified into 3 main categories: clear, partially cloudy and overcast [3]. Perez et al simulated power output of PV system using 2 different types of input: satellite-derived and ground measurement of solar irradiance. The result of comparing satellite-derived database with ground measurement suggests that even though there is a high deviation in an hourly basis, the overall bias was negligible for an annual term [4]. Also, Man et al used software called "Solar analyst" which requires surface information data to calculate the potential of installing photovoltaic (PV) modules on unused rooftops in Hong Kong. The spatial join technique is applied to combine solar irradiance map and terrain structure map to demonstrate the optimal rooftops for installing PV modules [5].

Although these works are similar to this study in a sense of assessing solar irradiance by means of satellite data tuned by ground measurements, there is no publication available which estimated solar resource over Mongolia by using satellite data. Therefore, this study is the first try to apply satellite data to Mongolian solar energy sector and expected result is more likely to the research outcomes presented by J.Alonso-Montesinos et al [3] because the goal of both of these studies is same which is to estimate solar resource from satellite data. But there are some differences due to the different satellite sensors and climate dissimilarity between EU and Mongolia. After assessing solar resource of Mongolia, it is possible to extend this research to simulate the output of solar power plant or to choose the most profitable locations for specific solar technologies as results presented by Perez et al and Man et al [4-5].

II. THE DATA BASE

A. Satellite data.

Himawari 8/9 are identical Japanese GMS and were launched in 2014 and 2016, respectively. It rotates

* Electronic address: onon.b@seas.num.edu.mn

in a geostationary orbit which means its rotational speed and direction is the same as earth's; thus, to ground observers, it appears motionless at a fixed position in the sky. The main sensor installed in Himawari 8 satellite is called Advanced Himawari Imager (AHI) which is capable of taking snapshots in total 16 spectral bands from which the first 3 are in visible, the following 3 are in Near Infrared (NIR) and the rest are in Infrared (IR) range of electromagnetic (EM) spectrum as shown in Table 1. The spatial resolution is 0.5-1 km for visible range and 1-2 km for NIR and IR range. Visible channel data are used in this study which are focused on blue, green and red colors with wavelengths of 0.46 µm, 0.51 µm and 0.64 µm, respectively. The data provided by Himawari 8/9 is in NETcdf format which stores multidimensional scientific meteorological data from which surface albedo is the parameter of main importance.

Table 1. Technical specifications of Himawari 8/9.

Band No	EM spectrum	Spatial resolution (km)	Wavelength (µm)
1	Visible	0.5-1	0.46
2			0.51
3			0.64
4	Infrared	1-2	0.86
5			1.6
6			2.3
7	Near Infrared		3.9
8			6.2
9			7.0
10			7.3
11			8.6
12			9.6
13			10.4
14			11.2
15			12.3
16			13.3

B. Ground measurement data

Figure 1. Locations of ground truth weather stations.

The ground measurement data of solar irradiance has two major importance. First, ground data is used to derive the optimal values of transmission coefficient τ and correction coefficient α which are input parameters to the semi-physical solar irradiance estimation model proposed in this study. Second, ground data is necessary to evaluate the model performance. It is also essential to check the quality of ground measurement data because input parameters and accuracy of the model would be determined by comparing satellite estimation with ground measurement. Thus, sensors should be calibrated carefully and operation and maintenance (OM) should also follow the approved standards.

Table 2. Detailed information about ground measurement sites.

No	Location	Latitude	Longitude	Period
m1	National University of Mongolia, Ulaanbaatar	47.92	106.92	2018/04-2018/10
m2	5 Buudal, Ulaanbaatar	47.94	106.90	2015/11-2016/04
m3	Choibalsan, Dornod	48.06	114.51	2016/01-2016/12
m4	Durgun, Khovd	48.34	92.47	2016/01-2016/12

As pinpointed in Figure 1 and listed in Table 2, the number of ground-based weather stations used in this study is limited. Measurement site m1, m2 and m4 are located in central and western Mongolia, respectively and are properties of National University of Mongolia (NUM). Measurement site m3 is in the eastern part of the country and is managed by Information and Research Institute of Meteorology Hydrology and Environment (IRIMHE), Mongolia. These ground measurement locations are chosen in such a way that it can be used to represent the local solar climate of western, central and eastern parts of Mongolia. Ground weather station measures not only global horizontal irradiance (GHI) but also several other meteorological parameters such as ambient temperature, relative humidity, wind direction and speed.

III. METHODOLOGY

In general, solar radiation models are divided into 3 main groups: empirical, physical and semi-physical models. The empirical models are based on the relation between satellite observation and ground measurement data while physical models calculate surface radiation only from satellite data by means of radiative transfer. A semi-physical model is a hybrid approach which is somewhere between empirical and physical models [2]. The foundation of it is just the same as physical models but it acts as an empirical model in a way that some input parameters are obtained by correlating satellite data with ground measurement.

In this study, solar resource of Mongolia is estimated by the semi-physical model which calculates solar irradiance by means of ground albedo [6]. By using visible channel images from satellite data, ground albedo could be observed neatly in various environments throughout the year. It is the main advantage of this model because the ground albedo changes over time and location.

As depicted in Figure 2, solar irradiance is attenuated and absorbed by atmospheric gases and clouds while it is traveling through the atmosphere. When it reaches the surface of the earth, some part is reflected back into the atmosphere by the ground albedo. Planetary albedo which is the average reflectance of earth constitutes of ground, atmospheric and cloud albedo and is observed by satellite. Thus, it is assumed that the ground albedo should be the minimum value of planetary albedo because the reflectance of the surface is usually lower than that of clouds [6]. This can be written as Equation 1.

$$H = \frac{I_0 * \cos(1-z) * (\tau * m - \rho_p * \alpha)}{1-\rho_s} \quad (1)$$

where:

H – Global Horizontal Irradiation (GHI)

I_0 – solar constant (1370 W/m²)

z – solar zenith angle

τ – transmission coefficient

m – airmass

ρ_p – planetary albedo

α – correction coefficient

ρ_s – ground albedo

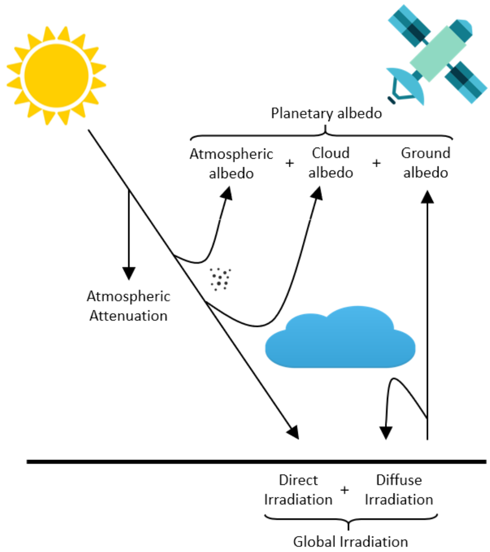

Figure 2. Illustration of the semi-physical model.

The optimum value of transmission and correction coefficients are derived by correlating satellite data with ground measurements. Time series value of airmass and zenith angle are calculated by solar position algorithm which only requires given time of a year and geographical location.

The flowchart of model implementation is shown in Figure 3. First of all, concurrent satellite and ground measurement data are correlated to obtain the optimal values of transmission and correction coefficients by means of Look up Table (LUT) where they should be in the inclusive range of [0,1] and those are not in this limit should be filtered.

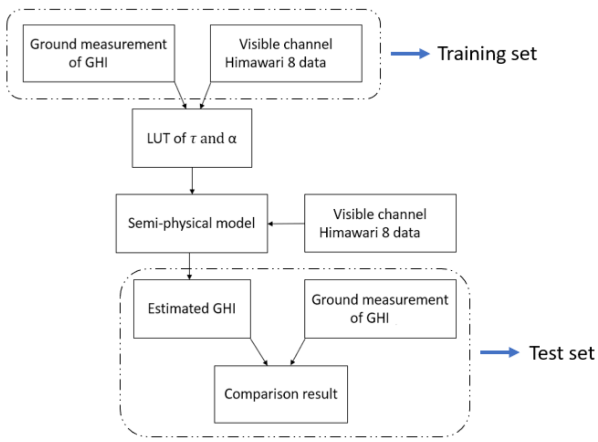

Figure 3. Flowchart of model implementation.

Moreover, they are computed to achieve the minimum root mean square error (RMSE) between measurement and estimation. Then, these LUT along with satellite data is input to the semi-physical model and the output will be the estimated value of GHI. Finally, estimation should be compared with the ground measurement to demonstrate the model's performance. It should be noted that ground measurements are divided into 2 groups: one for training and other for testing. The comparison results will be expressed in statistics of mean bias error (MBE), RMSE and correlation coefficient.

IV. RESULTS

A. Estimation of ground albedo

It is assumed that ground albedo should be the minimum value of satellite data. Figure 4 displays visible channel data retrieved from Himawari 8 satellite for Ulaanbaatar in 2016. Red circles are minimum values of these data for every month and thus regarded as a monthly ground albedo.

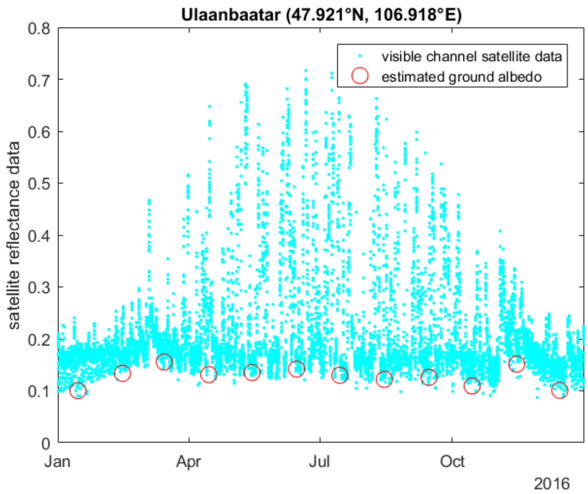

Figure 4. The minimum value of satellite data as a ground albedo.

Table 3. Estimation of monthly ground albedo in 2016.

Location / Month	Ulaanbaatar (m1 and m2)	Choibalsan, Dornod (m3)	Durgun, Khovd (m4)
Jan	0.1003	0.1635	0.0485
Feb	0.1335	0.1834	0.1079
Mar	0.1554	0.1558	0.1814
Apr	0.1313	0.1349	0.1772
May	0.1352	0.1243	0.1408
Jun	0.1419	0.1254	0.1451
Jul	0.1297	0.1327	0.1622
Aug	0.1219	0.1126	0.1268
Sep	0.1259	0.1087	0.1217
Oct	0.1092	0.0926	0.14
Nov	0.1514	0.2088	0.1
Dec	0.1009	0.1405	0.0537

It can be seen that during the cold season, reflectance data dotted as cyan do not change much because of the continuous snow cover. But it varies greatly during warmer months because the ground surface is no more covered by the highly reflective snow. This resulted in a high variation between minimum and maximum values of reflectance data where minimums and maximums represent ground albedo and cloud albedo, respectively. Monthly ground albedo values of 2016 are calculated not only for Ulaanbaatar but also for site m3 and m4 and can be found in Table 3. For these locations, the calculated ground albedo shows a similar trend as Ulaanbaatar.

B. Estimation of GHI

Solar irradiation over Ulaanbaatar is estimated by the semi-physical model for the period of 2018/04/03 to 2018/05/09. Ground measurement data of site m2 and m1 are used for deriving model parameters and conducting uncertainty assessments of the model performance, respectively. The scatter plot between the estimation and measurement of GHI is shown in Figure 5 where the red line is 1 by 1 line. Although there are some outliers from 1 by 1 line, most of the time, data points reside closely to it.MBE, RMSE and correlation coefficient r are found to be -30.5 W/m2, 96.6 W/m2 and 0.91, respectively. Negative MBE means, on average, the radiation is estimated larger than it is actually measured. But it should be interpreted cautiously because positive and negative biases cancel each other.

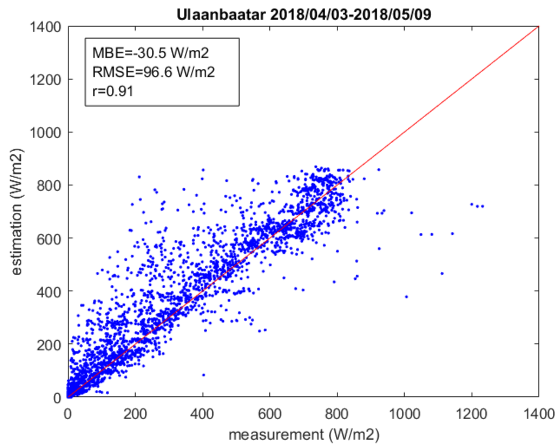

Figure 5. Estimated vs measured irradiance.

Thus, RMSE is chosen to describe the error between datasets since it is not sensitive to direction. Moreover, positive correlation coefficient r close to 1 is another statistic indicating good agreement

between 2 datasets. As a reference, in the study by Perez et al, hourly average RMSE was 95 W/m2 for the GHI component [7] which describes the current model's compatibility with other available models.
Model performance is investigated on different sky conditions classified as clear, cloudy and overcast. From the left panel of Figure 6, it can be seen that estimated horizontal radiation agrees very well with ground measurement on clear days. However, on cloudy days as drawn on the middle panel, the model does not estimate surface radiation correctly owing to its incapability of capturing frequently changing sky condition. Because the temporal resolution of Himawari 8 satellite is 10 minutes, it cannot detect changes which last shorter than 10 minutes. Moreover, it is unusual that GHI reached up to 1200 W/m2 around noon of 2018/04/13 because even on clear sky days like 2018/05/01, the maximum value of GHI was around 800 W/m2. This phenomenon can be explained by cloud induced Radiation Enhancement (RE) which occurs often in presence of broken clouds. Because of cloud inhomogeneity, there are occasions that measured surface radiation exceeds the supposed clear sky radiation. Current satellites are not capable to obtain the cloud structure in 3 dimension (3D) which points the necessity of development of 3D models for solar irradiance estimation [8]. Finally, model behavior on overcast days is illustrated on the right panel where it overestimates ground level solar radiation.

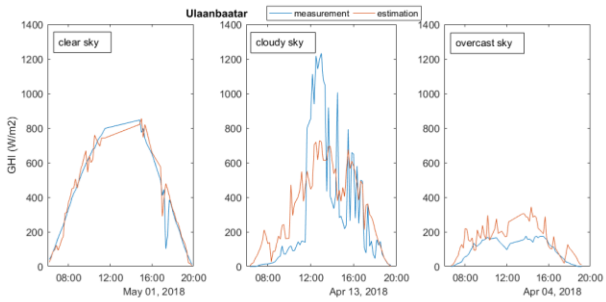

Figure 6. Measured and estimated GHI under different sky conditions.

C. Monthly and annual average solar maps

Daily sum of solar energy is averaged into a monthly and annual value and mapped for the year 2016. Figure 7 displays the monthly average daily sum of GHI. Daily total GHI values in winter months are approximately 2 kWh/m2/day shown in pale yellow which is significantly lower than that of summer months when it reaches up to 7 kWh/m2/day displayed by deep red. This is because the day length is shorter in winter and longer in summer in the northern hemisphere.
Figure 8 is the map of annual average daily solar energy received in Mongolia in 2016. Because available solar energy depends highly on the geographical location, the sun shines in an angle closer to 90 degree in locations closer to equator while the angle between the solar disk and the horizontal surface becomes more slant towards poles due to the revolution mechanism of the earth in relation to its sphere shape and tilted axis. This results in that the southern part of Mongolia, also known as Gobi-desert yields more solar energy (4kWh/m2/day) compared to the northern part (3.5kWh/m2/day).
It should be noted that these monthly and annual average solar maps are results of analyzing only one-year satellite observation data. In order to reduce the uncertainty resulting from spatial and temporal variability of solar radiation, it is highly recommended to record the data as many years as possible and average that values. Nevertheless, this one-year average daily GHI map agrees with the results presented by IRENA [1] which acclaims that the daily average solar energy in Mongolia is 3.4-5.4 kWh/m2/day.

V. CONCLUSIONS

This study evaluates the solar potential of Mongolia by means of ground albedo derived from visible channel data of Himawari 8 satellite. The estimated solar radiation is checked against ground truth measurement in Ulaanbaatar City for the period of 2018/04/03 to 2018/05/09. As a result, MBE, RMSE and correlation coefficient were -30.5 W/m2, 96.6 W/m2 and 0.91, respectively. Furthermore, it is found that model works well on clear sky days but tends to underestimate under broken clouds condition and overestimate on overcast days. Finally, the solar potential map of Mongolia is drawn by integrating GHI values on a daily basis and averaging it for a month and a year. It is found that Mongolia received 3.5- 4.5kW h/m2/day solar energy on an average day of 2016 which generally agrees with the results published by IRENA. Therefore, it shows the effectiveness of utilizing satellite data to monitor solar energy on a large scale when the number of ground measurement stations is not sufficient.

It is found that the semi-physical model does not correctly estimate surface solar irradiation in the presence of clouds. Because the underestimation is caused by RE effect, designing a 3D model to capture cloud properties may lead to improvement. On the other hand, the overestimation behavior can be fixed by training the model with extensive data sets of ground measurement and corresponding satellite observation. Since the current model is not designed to receive IR band data as input, it is highly susceptible to the failure of distinguishing cloud over snow covered areas. Therefore, the current study can be extended by utilizing additional IR channels to distinguish highly reflective objects due to their temperature.

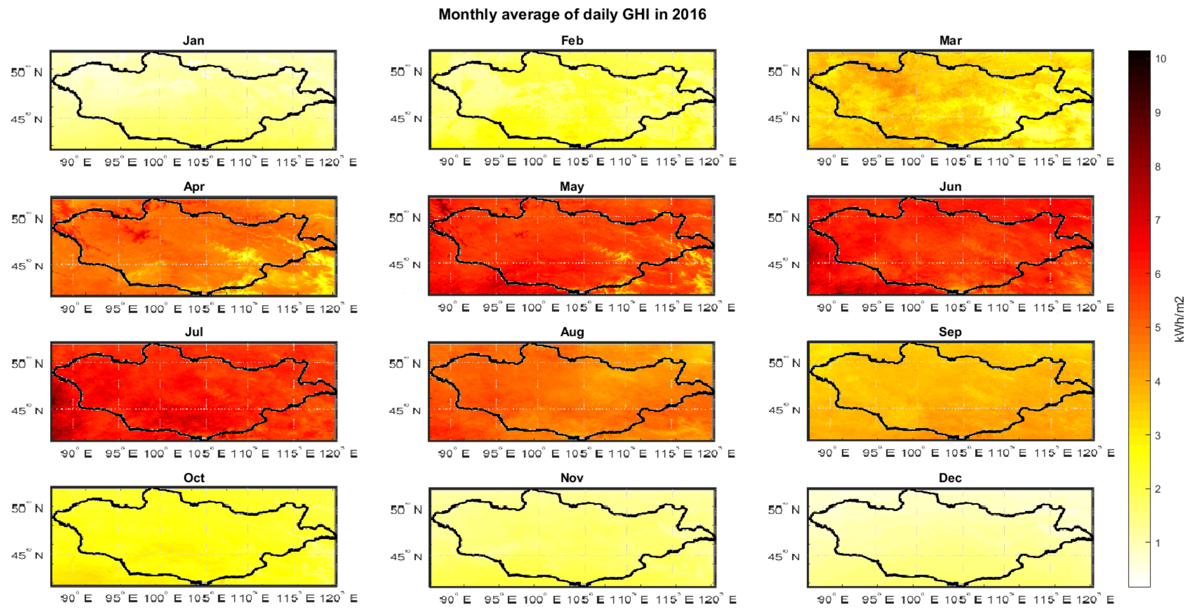

Figure 7. Monthly average daily GHI map of Mongolia.

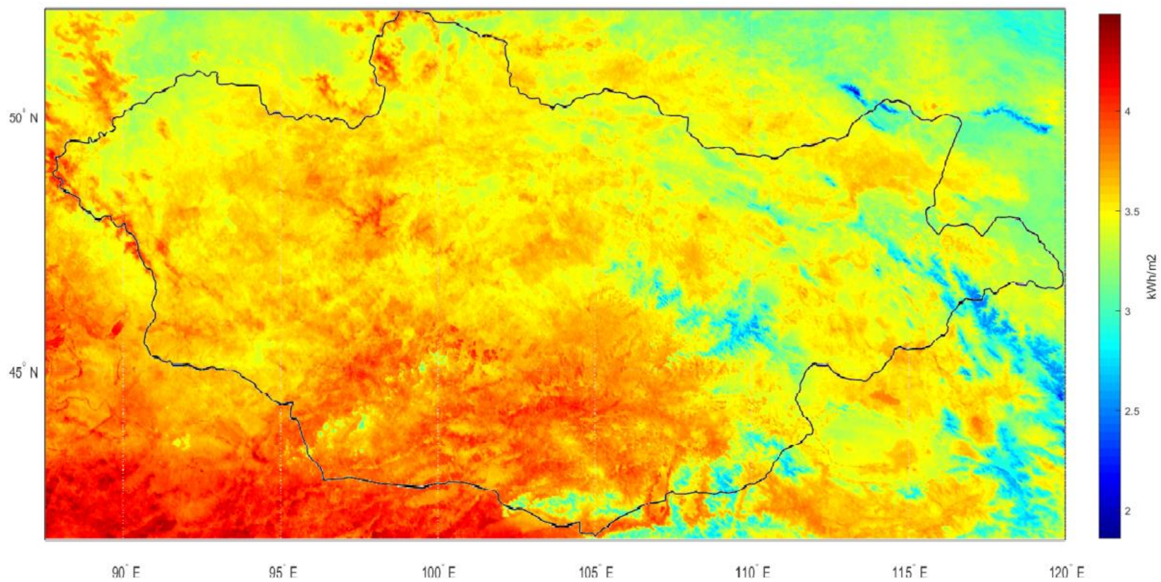

Figure 8. Annual average daily GHI map of Mongolia in 2016.

VI. REFERENCES

[1] "Mongolia-renewables readiness assessment," International Renewable Energy Agency /IRENA/, Tech. Rep.

[2] M. Sengupta, A. Habte, S. Kurtz, A. Dobos, S. Wilbert, E. Lorenz, T. Stoffel, D. Renné, C. Gueymard, S. Wilcox, P. Blanc, and R. Perez, "Best practices handbook for the collection and use of solar resource data for solar energy

applications," National Renewable Energy Laboratory, United States Department of Energy, Tech. Rep., 2015.

[3] J. Alonso-Montesinos, F. Batlles, and J. Bosch, "Beam, diffuse and global solar irradiance estimation with satellite imagery," Energy Conversion and Management, vol. 105, pp. 1205–1212, 2015.

[4] J. S. Stein, R. Perez, and A. Parkins, "Validation of PV performance models using satellite-based irradiance measurements: A case study." ASES National Solar Conference, 2010.

[5] M. S. Wong, R. Zhu, Z. Liu, L. Lu, J. Peng, Z. Tang, C. H. Lo, and W. K. Chan, "Estimation of Hong Kong's solar energy potential using GIS and remote sensing technologies," Renewable Energy, vol. 99, pp. 325–335, 2016.

[6] K. Otani, K. Kurokawa, I. Tsuda, T. Saitoh, and T. Horigome, "Estimation of ground aldebo by gms images for solar irradiation monitoring," Solar Energy Materials and Solar Cells, vol. 35, pp. 395–400, 1994.

[7] R. Perez, M. Kmiecik, K. Moore, S. Wilcox, R. George, D. Renné, F. Vignola, and P. Ineichen, "Status of high-resolution solar irradiance mapping from satellite data."

[8] A. Damiani, H. Irie, T. Horio, T. Takamura, P. Khatri, H. Takenaka, T. Nagao, T. Y. Nakajima, and R. R. Cordero, "Evaluation of himawari-8 surface downwelling solar radiation by skynet observations," Atmospheric Measurement Techniques, 2017.